Konya Mühendislik Bilimleri Dergisi, c. 12, s. 1, 373-395, 2024
Konya Journal of Engineering Sciences, v. 12, n. 1, 373-395, 2024
ISSN: 2667-8055 (Electronic)
DOI: 10.36306/konjes. 1419225

HEAT TRANSFER EXAMINATION OF OSCILLATING NANOFLUID FLOW IN A RECTANGULAR CORRUGATED CHANNEL WITH VERTICAL PLATES: A NUMERICAL STUDY

Selma AKÇAY

Çankırı Karatekin University, Engineering Faculty, Mechanical Engineering Department, Çankırı, TÜRKİYE
selmaakcay@karatekin.edu.tr

Highlights

- The heat transfer of pulsating nanofluid flow in a rectangular corrugated duct with vertical plates.
- Effects of pulsating flow, vertical plates, Al_2O_3-water nanofluid, and Reynolds number.
- Nu increased by 1.57 times for the oscillating nanofluid flow at a Re = 800 in the duct with plates.

Graphical abstract

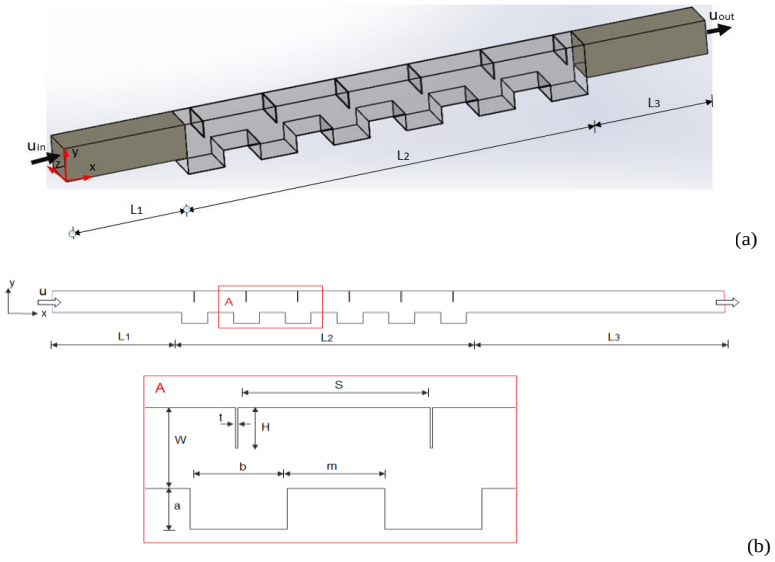

(a) 3D, and (b) 2D geometric schematics of the numerical model

***Corresponding Author:** Selma AKÇAY, selmaakcay@karatekin.edu.tr

Konya Mühendislik Bilimleri Dergisi, c. 12, s. 2, 373-395, 2024
Konya Journal of Engineering Sciences, v. 12, n. 2, 373-395, 2024
ISSN: 2667-8055 (Electronic)
DOI: 10.36306/konjes.1419225

HEAT TRANSFER EXAMINATION OF OSCILLATING NANOFLUID FLOW IN A RECTANGULAR CORRUGATED CHANNEL WITH VERTICAL PLATES: A NUMERICAL STUDY

Selma AKÇAY

Çankırı Karatekin University, Engineering Faculty, Mechanical Engineering Department, Çankırı, TÜRKİYE
selmaakcay@karatekin.edu.tr

(Received: 13.01.2024; Accepted in Revised Form: 29.02.2024)

ABSTRACT: This study numerically focused investigating the thermal performance of flow oscillations in a rectangular corrugated channel with vertical plates on top wall. The numerical study was performed with the ANSYS Fluent software, and the SIMPLE algorithm was utilized to solve the pressure-velocity coupling. The top wall of the channel was adiabatic and included vertical plates. The bottom wall of the channel was rectangular grooved and kept at T_w=360 K. Suspension of Al_2O_3 nanoparticles into water was used as the fluid. The particle volume fraction in the suspension was kept constant at φ = 5%. Oscillating amplitude (A) and Strouhal number (St) were maintained constant at A = 1 and St = 2, respectively. In the presented study, the effects of vertical plates, Al_2O_3-water nanofluid and pulsating flow on flow and heat transfer were analyzed separately at different Reynolds numbers ($200 \leq Re \leq 800$). The Nusselt number (Nu), relative friction factor (f_{rel}) and performance evaluation criteria (PEC) were obtained for different Reynolds numbers. The temperature and velocity fields were acquired for varying parameters. The results demonstrated that the flow and temperature structures were significantly influenced by the channel geometry and oscillating flow. Heat transfer considerably enhanced with the oscillating flow at the high Re. At Re = 800, thermal improvement for oscillating flow of the nanofluid in the channel with plates increased by nearly 1.57 times relative to the steady case of the basic fluid in the channel without plates.

Keywords: *Heat transfer, Nanofluids, Oscillating flow, Rectangular corrugated channel, Vertical plate*

1. INTRODUCTION

Corrugated channels are a widely used passive heat transfer improvement method. Since these channel geometries increase the surface area and create an oscillating motion in the flow, they have significant potential for heat transfer improvement. This method does not contain any mechanical parts, so it is more economical and quite safe. Therefore, it is usually preferred in many engineering implementations such as thermal devices, heat exchangers, and chemistry processes [1-3]. In many experimental and numerical studies, the hydraulic and heat transfer enhancement has investigated in the corrugated channels, and the results of these studies demonstrated that wavy surface geometries significantly improve heat transfer when compared to straight channels [4-6]. Kurtulmus and Sahin [7] actualized a review study investigating the hydraulic and thermal characteristics on corrugated surfaces. In experimental and numerical work, Brodnianská and Kotśmíd [8] examined the thermal improvement in a duct with various wave forms and demonstrated that the thermal enhanced with the increasing Re and decreasing channel height. Mehta et al. [9] computationally examined the impacts of the wall wave amplitude on flow and thermal improvement in asymmetrical corrugated channels and declared that the Nu increased with Re and wall wave amplitude.

Another passive heat transfer improvement techniques are the use of extended surface modifications, such as twist tape, winglets, ribs, fins, barriers, and plates within the channel. These modifications added into the channel completely disrupt the flow structure and help with the flow mix and thermal improvement, but an increase in pressure loss occurs relative to straight ducts. Many experimental and numerical works have examined the flow and thermal enhancement in grooved and

***Corresponding Author:** Selma AKÇAY, selmaakcay@karatekin.edu.tr

straight channels with different barriers [10-11]. Barriers with different shapes in different channel geometries have been investigated in previous studies. Lei et al. [12] examined the inclination angle of the baffles on thermal efficiency in a heat exchanger with helical turbulators. Sripattanapipat and Promvonge [13] numerically investigated the heat transfer of a duct with diamond-type barriers. Kwankaomeng and Promvonge [14] executed a numerical study investigating thermo-hydraulic behavior in a square duct with 30° inclined barriers on one surface. Sriromreun [15] performed a numerical work on the thermo-hydraulic behavior of inclined barriers in a rectangular channel. Li and Gao [16] numerically studied thermal enhancement in a triangular-shaped grooved duct with delta-type baffles. Karabulut [17] realized a CFD (Computational Fluid Dynamics) work studying the heat transfer at different slope angles of the baffles in a triangular corrugated duct, including triangular barriers on the upper wall. In a computational and experimental research, Bensaci et al. [18] studied the thermal efficiency of solar air channels with varying baffle configurations. These study results showed that corrugated/wavy ducts and surface arrangements considerably enhanced the thermal performance. In an experimental study, Promvonge et al. [19] researched the heat transfer in a duct with inclined horseshoe-type barriers and noticed that the heat transfer improved by nearly 208% and the pump power increased about 6.37 times, according to the flat duct. Kumar et al. [20] experimentally examined the thermal improvement of the solar duct with multiple V-shaped baffles. They declared that the thermal enhancement exceedingly increased with the baffles. In another experimental work conducted by Sahel et al. [21] was reported the rectangular channel flow with a different arrangement of the barriers increased the heat transfer about 65%.

On the other hand, the thermo-physical features of many traditional liquids utilized in heat transfer implementations are low. Particles with nano-sized are added to enhance these features of a basic fluid. Many researchers have examined nanofluids together with corrugated ducts [22-24]. Manca et al. [25] examined the thermal characteristics of water based Al_2O_3 nanofluid for different particle volume fractions ($0 \leq \varphi \leq 0.04$) in a duct with varying rib heights and declared that thermal performance improved with increasing the Re and φ. They also observed a rise in the pump power. Heshmati et al. [26] investigated the heat transfer efficiency of nanofluids in a duct with different geometries of the barriers. Their study examined the effects of nanofluid type, particle volume fraction ($0.01 \leq \varphi \leq 0.04$), particle diameter, and Reynolds number ($40 \leq Re \leq 400$). They found that the nanofluids with high particle volume ratio and small particle size enhanced thermal performance. In a review study, Huminic and Huminic [27] analyzed the thermal behavior of nanofluids and basic fluids in the grooved channel. Qi et al. [28] numerically and experimentally researched the thermal behavior of the nanofluids (TiO_2-water) in a grooved channel. Pordanjani et al. [29] presented review work that examined the impacts of nanoparticles on energy savings in heat exchangers. Mei et al. [30] theoretically studied the thermohydraulic performance of Fe_3O_4-water nanofluid using a magnetic field in a wavy channel. Kaood and Hassan [31] presented a theoretical work that analyzed the thermal improvement and energy analysis of varying nanofluids in different geometries of the wavy duct. They indicated that nanofluids enhanced the thermal performance according to the straight channel, and all the performance improvement decreased at $Re \geq 10000$ for all the fluids and channel configurations. Tian et al. [32] analyzed the energy, exergy analysis, and pump power of the triangular turbulators in different duct geometries. In their study, they examined the effects of different fluid types (CuO-water, Al_2O_3-water, water, and air). As a result of their study, they declared that the heat transfer was considerably enhanced in nanofluid flow in circular channels with turbulators. However, the nanofluids increased exergy destruction. Ajeel et al. [33] performed a numerical study that examined the thermal behavior of ZnO-water nanofluid in a curved wavy duct with L-type barriers. They indicated that the nanofluids and barriers had an important influence on thermal improvement. Akcay [34] evaluated the heat transfer of pulsating flow in a duct with inclined baffles for different Reynolds numbers, pulsating frequency, and pulsating amplitude. The result of the study indicated that the thermal performance improved by about 47% with increasing Reynolds number and pulsating parameters. Menni et al. [35] evaluated the thermal characteristics of baffles at varying angles in a channel under nanofluid flow. Their study results

indicated that the heat transfer enhanced at a high Re, and the highest thermal enhancement was obtained for the vertical baffles.

Although extended surfaces added to the channel and corrugated channel geometry increase heat transfer under steady flow conditions, these applications are insufficient in cases where higher thermal performance is required. For this reason, in these cases, a pulsating/oscillating flow is preferred over a steady regime. An oscillating flow enhances thermal performance by improving the flow mixing. Many experimental and numerical works have investigated the thermo-hydraulic efficiency in the wavy ducts under oscillating flow. The results of these studies indicated that the heat transfer enhanced depending on the geometry of the duct, the velocity of fluid, and oscillating parameters [36-38]. In two different numerical studies, Akdag et al. examined the thermal enhancement of the oscillating nanofluid flow in a triangular [39], and trapezoidal [40] corrugated channels. They indicated that the thermal enhancement increased with a rising oscillating frequency, oscillating amplitude, and particle volume ratio. Esfe et al. [41] executed a review work investigating the oscillating flow for heat transfer and non-heat transfer conditions. Munoz-Camara et al. [42] experimentally examined the thermal efficiency in the oscillating flow in a circular duct with barriers and declared that the heat transfer increased nearly five times with the oscillating flow. Akcay [43] presented a CFD work to investigate the heat transfer of the flow oscillations in a grooved duct with V-shaped winglets and found that the winglets and pulsating flow significantly increased thermal enhancement with rising in pump power. In another numerical study, Akcay [44] examined the pulsating flow of CuO-water nanofluid in a circular corrugated channel with barriers on the top wall. The results were compared with the steady case of the basic fluid in the non-barriers corrugated channel. The work's findings indicated the pulsating nanofluid flow improved the Nu by 2.6 times in the presence of baffles.

According to the above research, extended surfaces added to corrugated channels increase the thermal enhancement. Even if the heat transfer with these modifications is enhanced, the pressure loss rises due to the nanoparticles and obstruction of the flow area. A definite criterion has not been reported for determining the optimum nanofluids and corrugated channel geometries with plates in the existing literature. Thermal and hydraulic behavior in corrugated channels with plates were mostly studied under steady flow conditions, and it was found that very little study was realized under oscillating flow conditions. In studies carried out so far, it has been observed that thermal and hydraulic performance in oscillating nanofluid flow in a rectangular corrugated channel with vertical plates has not been examined. In the study, the impacts of vertical plates, nanofluids, and oscillation parameters on thermal enhancement and pressure drop in rectangular corrugated channels were analyzed separately.

2. MATERIAL AND METHODS

2.1. Numerical Geometry

Figure 1 indicates the geometry of the rectangular corrugated channel with vertical plates on the top surface. The height of the channel (W) is 12 mm. The channel width (Z) is equal to channel height. The lengths of flat parts at the inlet and exit of the channel are considered as L_1 = 5 W and L_3 = 10 W, respectively. The distance between plates is S = 3 H. The thickness and the length of plates are t = 0.05 W and H = 0.5 W, respectively. The distance between corrugated parts is m = 0.5 W. The dimensions of the corrugated part are a = 0.5 W and b = W. The corrugated channel contains a total of six wavy parts.

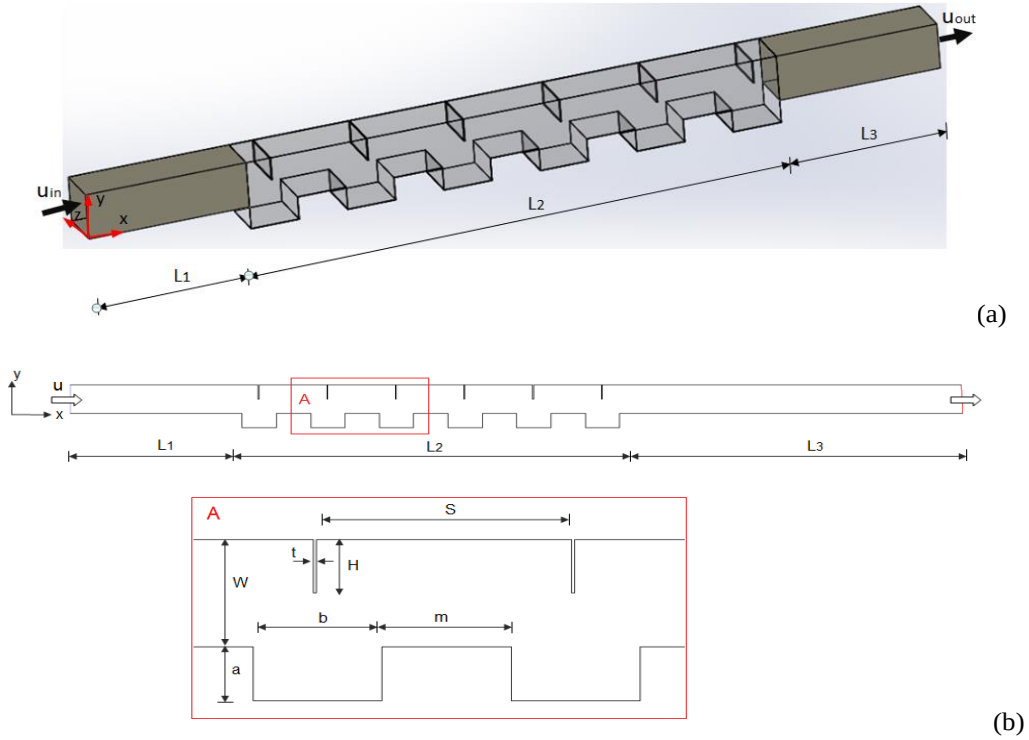

Figure 1. (a) 3D, and (b) 2D geometric schematics of the numerical model

2.2. Mathematical Model

In the numerical solutions, the flow field is laminar, time-depended for oscillating flow, steady for the other cases, two-dimensional (2D). The fluid is incompressible and Newtonian type. The impacts of thermal radiation and body forces are ignored. For these conditions, the continuity equation conservation, momentum, and energy equations are given as [36]:

$$\frac{\partial u_i}{\partial t} + \nabla(\rho u) = 0 \tag{1}$$

$$\frac{\partial u_i}{\partial t} + \frac{\partial (u_i u_j)}{\partial x_i} = -\frac{\partial P}{\partial x_i} + \frac{1}{Re}\nabla^2 u_j \tag{2}$$

$$\frac{\partial T}{\partial t} + u_i \frac{\partial T}{\partial x_i} = \frac{1}{RePr}\nabla^2 T \tag{3}$$

Reynolds number (Re) is given by [43]:

$$Re = \frac{\rho u D_h}{\mu} \tag{4}$$

Hydraulic diameter (D_h) is calculated as follows (Eq. 5) [44]:

$$D_h = \frac{4A_c}{P} = \frac{4WZ}{2(W+Z)} \tag{5}$$

where A_c denotes the cross-sectional area and P denotes the wetted perimeter.

The oscillating frequency (Strouhal number, St) is given by [36]:

$$St = \frac{\omega D_h}{u} \tag{6}$$

2.3. Description of Boundary Conditions

The fluid enters the channel at T_i = 300 K. The rectangular corrugated lower wall of the channel is preserved at 360 K. The "velocity inlet" and "pressure outlet" boundary conditions are identified at the inlet and outlet of the channel, respectively. The oscillating inlet velocity defined at the channel inlet is given by Eq. (7) [36, 43].

$$u_{in} = u[1 + Asin(\omega t)] \tag{7}$$

where, ω (= 2πf) is defined as the angular velocity and is used to obtain the Strouhal number (St), which describes the dimensionless oscillating frequency, A represents the dimensionless oscillating amplitude, and u indicates the mean velocity at the channel inlet. L_1 and L_3 lengths have adiabatic and no-slip conditions. Also, the vertical plates have adiabatic and no-slip conditions. The simulations are applied for different Reynolds numbers (Re: 200, 500, and 800). The study is carried out under laminar flow conditions. It was reported that the transition from laminar to turbulent flow in pulsating flow begins at Re=1100. Therefore, in this study, Reynolds numbers in the range of 200<Re<800 were used to maintain the validity of laminar flow conditions (for detailed information, see [34]).

2.4. Data Reduction

In this study, heat transfer is expressed with the Nusselt number (Nu). The overall Nusselt number for steady conditions is written as [34]:

$$Nu = \frac{hD_h}{k_f} \tag{8}$$

$$h = \frac{Q_{conv}}{A_L \Delta T_{lm}} \tag{9}$$

$$Q_{conv} = mC(T_{o,b} - T_{i,b}) \tag{10}$$

$$\Delta T_{lm} = \frac{(T_{i,b} - T_{o,b})}{ln\left(\frac{T_w - T_{o,b}}{T_w - T_{i,b}}\right)} \tag{11}$$

where, k is the heat conductivity, h is the heat convective coefficient, and ΔT_{lm} is logarithmic temperature difference. $T_{i,b}$ and $T_{i,o}$ represent the bulk temperature of the fluid at inlet and outlet of the channel, respectively. T_w shows the wall temperature of the corrugated channel. C, A_L, Q_{conv}, and m are the specific heat, surface area, heat transfer with convection, and, mass flow rate, respectively.

The overall Nusselt number (Nu_p) for oscillating flow conditions can be written as [36]:

$$Nu_p = \frac{1}{\tau L} \int_{x_o}^{L} \int_{0}^{\tau} Nu(x,t) dt dx \tag{12}$$

where, τ indicates a period time in oscillating flow, L is the length of the heated corrugated channel.

The thermal enhancement ratio (Nu_{rel}) is found as [34]:

$$Nu_{rel} = \frac{Nu_p}{Nu_s} \tag{13}$$

where, Nu_p and Nu_s represent the cycle-averaged Nu for oscillating conditions, and the Nu for a steady condition, respectively.

The friction factor (f) is calculated by [43]:

$$f = \frac{2\Delta P D_h}{\rho u^2 L} \tag{14}$$

where, ΔP shows the pressure difference.

The relative friction factor (f_{rel}) is computed as [44]:

$$f_{rel} = \frac{f_p}{f_s} \tag{15}$$

where, f_s is the average friction factor for steady flow and f_p is the average friction factor for oscillating flow.

The performance evaluation criteria (PEC) is given by [43]:

$$PEC = \frac{(Nu_p/Nu_s)}{(f_p/f_s)^{1/3}} \tag{16}$$

2.5. Nanofluid Properties

In the study, Al_2O_3-water nanofluid was used as the fluid and the nanoparticle volume ratio was kept constant (φ = 5%). The diameter of the nanoparticles was accepted to be 20 nm. The thermodynamic features of the Al_2O_3-water nanofluid were calculated using the following equations [32, 45]:

$$\rho_{nf} = (1-\varphi)\rho_{bf} + \varphi\rho_{pt} \tag{17}$$

$$C_{nf} = \frac{(1-\varphi)\rho_{bf}C_{bf} + \varphi\rho_{pt}C_{pt}}{\rho_{nf}} \tag{18}$$

$$k_{nf} = k_{bf}\frac{[k_{pt}+2k_{bf}-2\varphi(k_{bf}-k_{pt})]}{[k_{pt}+2k_{bf}+\varphi(k_{bf}-k_{pt})]} \tag{19}$$

$$\mu_{nf} = \mu_{bf}[123\varphi^2 + 7.3\varphi + 1] \tag{20}$$

where the subscript *bf, pt and nf* show the basic fluid, the nanoparticle and the nanofluid, respectively. Water is used the basic fluid. Table 1 indicates the thermophysical properties of the basic fluid (water) and Al_2O_3 nanoparticle at 300 K [32].

Table 1 . Thermal and physical features of Al_2O_3 nanoparticle and H_2O at 300 K

	ϱ [kg/m³]	**C [J/kgK]**	**k [W/mK]**	**μ [kg/ms]**
H_2O	998.2	4182	0.6	0.001003
Al_2O_3	3950	765	36	-

2.6. Numerical Procedure and Validation

The 2D drawing of the channel geometry and the formation of the grid structure were generated with

the help of the Gambit software. The mesh quality for triangular elements of the numerical model was obtained as 0.94. Therefore, the triangular elements were preferred to both channels (with and without plates). The mesh structures of both channels are given in Figure 2 with their details. To determine whether the solution results were independent of the grid numbers, the Nu was obtained for different grid numbers, namely 34258, 54162, 77652, 105058, and 131604. Since the change in the Nu was very small after the 77652-element number, this element number was adapted to the geometry. Figure 3 illustrates the variations of the Nu with the grid numbers at different Re for the steady case in the rectangular corrugated channel without plates.

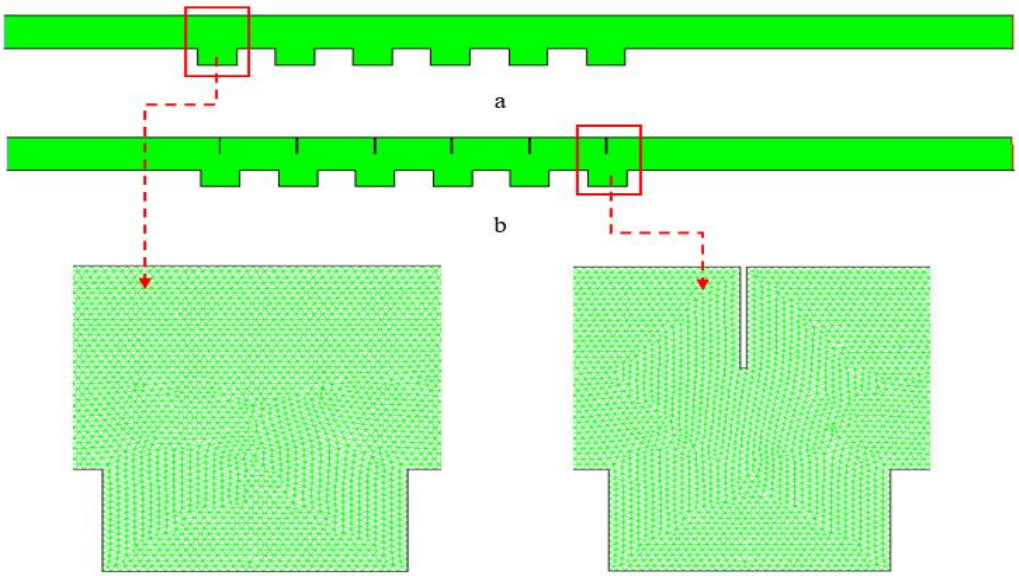

Figure 2. Mesh formations of the model: (a) without plates and (b) with plates

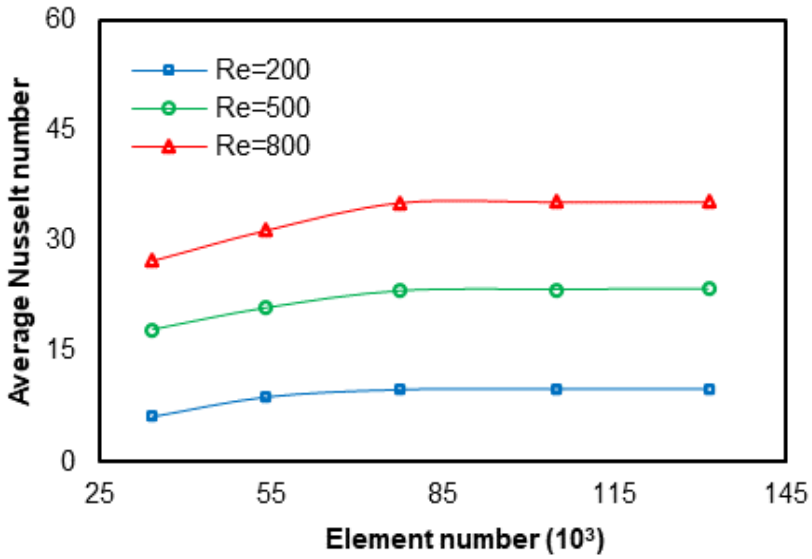

Figure 3. Nusselt numbers versus the element numbers for the steady case of the base fluid

The numerical simulations were realized by using the ANSYS Fluent [46] software. In the discretization of the relevant equations were used the second order upwind scheme. The velocity-pressure coupling in the discretized equations was solved with the SIMPLE algorithm. Convergence criteria were 10^{-8} for all the residuals. In oscillating flow, iterations were completed in 3000 s and then heat transfer and pressure drop calculations were performed.

Boukhadia et al. [47] studied the heat transfer and pressure drop for laminar flow in a straight channel with a hydraulic diameter of 12 mm. On the other hand, Ameur et al. [48] investigated convective heat transfer at Reynolds numbers in the range of $0.1 \leq Re \leq 300$ in a straight channel with the same hydraulic diameter. To validate the present simulation results, this work was checked with the results of the previous studies [47, 48]. The comparison of the numerical solutions of this study with the results of the previous studies was given detail in [43] and [44].

Time step independence test was carried out for three different time steps: Δt=0.1s, 0.01s, and 0.001s, and the test results were shown in Figure 4. Nusselt numbers were obtained very close to each other at time steps Δt=0.01s and Δt=0.001s. Therefore, the time step for oscillatory flow solutions was set to Δt=0.01 s.

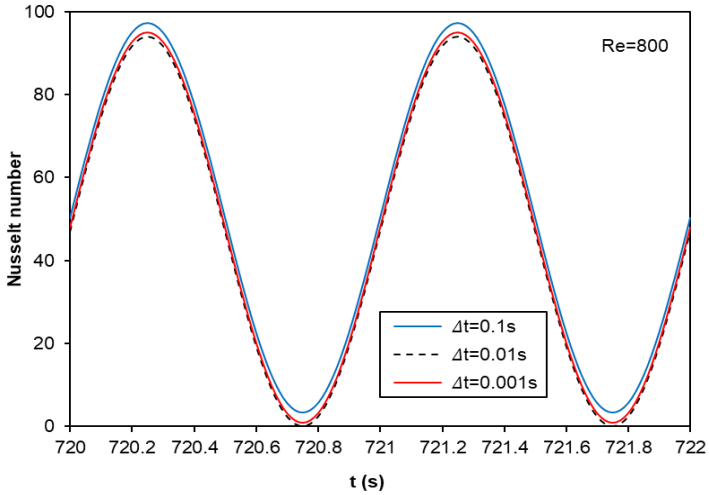

Figure 4. Time step independence test for Re=800

3. RESULTS AND DISCUSSION

In this section, the effects of vertical plates, Al_2O_3-water nanofluid and pulsating flow on flow and heat transfer were discussed for different Reynolds numbers ($200 \leq Re \leq 800$). In oscillating flow, the temperature and flow fields in the channel change with time and therefore, the pressure drop, and heat transfer will also change periodically. One oscillation period was utilized to compute the friction factor and Nu. One oscillating period was accepted to be completed in $\omega t = 360°$, or 2π radians. Moreover, the temperature and flow fields for the steady and oscillating cases of the flow in the channel with and without plates were presented. In the paper, color scale values for all velocity contours are given in m/s, and color scale values for all temperature contours are given in Kelvin (K).

Figure 5 indicates the velocity (a) and temperature contours (b) in the steady flow of the water in a rectangular corrugated channel without the plates for different Re. The velocity fields for the water in the channel without plates are like each other at all the tested Re. The fluid generally flows parallel to the channel walls and is canalized towards the rectangular cavities on the bottom wall (Fig. 5a). In the channel without plates, cold fluid flows in the upper parts of the channel. The length of corrugated channel is kept at a constant temperature, and the rectangular cavities were completely covered with hot fluid. The wall temperatures of the rectangular cavities near the inlet of the channel are relatively lower (first two rectangular cavities in the flow direction) while the temperature of the rectangular cavities towards the end of the channel was relatively higher (last four rectangular cavities in the flow direction). As the Re increased, the surface temperature of the rectangular corrugated channel reduced (Fig. 5b).

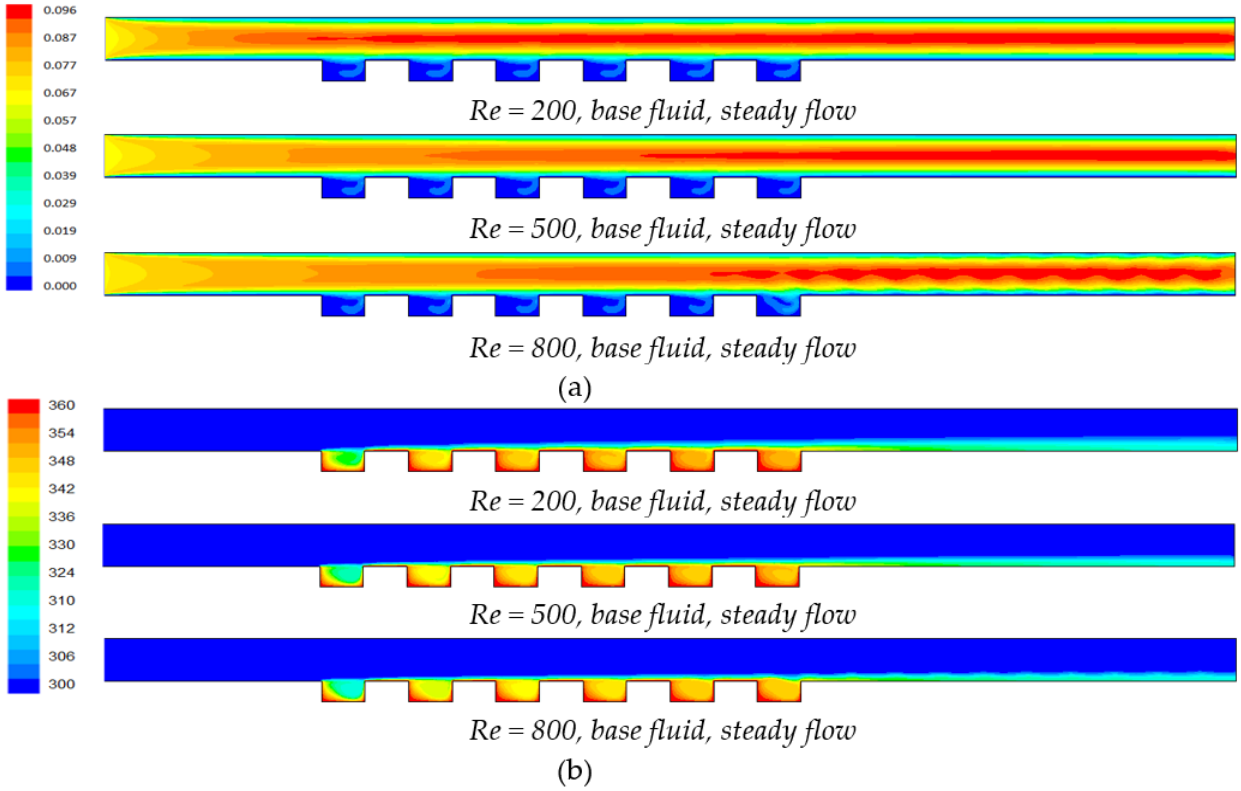

Figure 5. Velocity fields (a) and temperature fields (b) at different Re for the steady case of water in the corrugated channel without plates

Figure 6 indicates, the velocity contours (a) and temperature distributions (b) of the Al_2O_3-water nanofluid with $\varphi = 0.05$ particle volume fraction in the channel with plates for different Re in the steady case. The velocity and temperature contours significantly changed with the Re depending on the plates. The vertical plates significantly affected the flow field within the channel. These plates canalized the flow toward the rectangular corrugated surfaces, causing flow oscillation. With the oscillation movement, the cold fluid contacted the hot corrugated surfaces. The temperature of the corrugated walls in contact with the colder fluid decreased and the heat transfer improved. After each plate, the velocity and thermal boundary layer broke down and these structures helped to create flow cycles. The plates disrupted the flow structure, caused a diminish in thermal resistance, thus improving the heat transfer. At a low Re, it was seen that the flow cycles occurred between the vertical plates, while the mainstream flowed as a whole. With the increasing Re, flow breaks occurred and too many flow cycles were formed in the channel. The wall temperature decreased with the increasing Re.

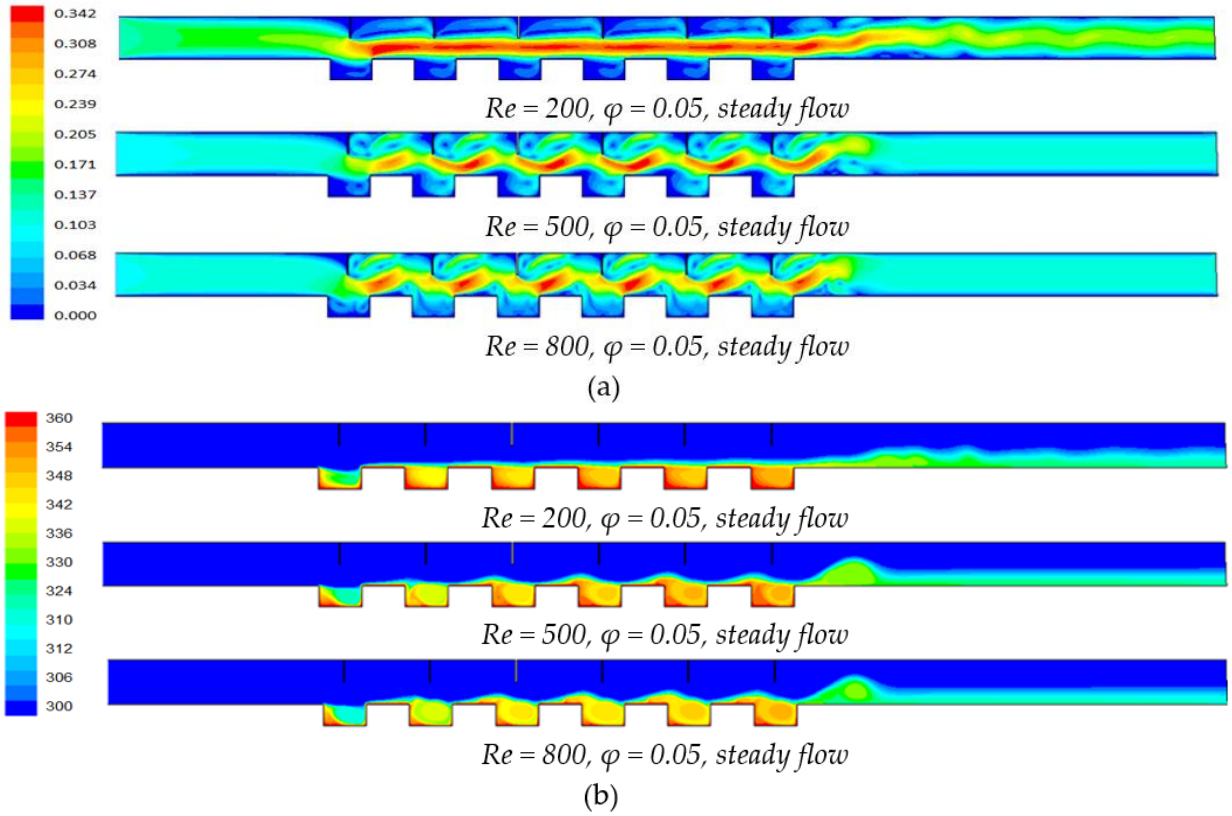

Figure 6. Velocity fields (a) and temperature fields (b) at different Re for the steady case of the nanofluid in the corrugated channel with plates

Figure 7 indicates the velocity vectors for different Re in the steady flow of nanofluid in the channel with plates. At a Re = 200, the velocity vectors for the main flow were downstream. It was seen that the velocity vectors between each plate were quite small and were positioned in different directions. In the rectangular cavities, the flow vectors were still small, and turbulence started in the flow. At a Re = 500, the oscillations occurred in the main flow due to the plates. Major and minor flow cycles were formed between each vertical plate. It was observed that a large flow cycle was formed near the right wall of each rectangular cavity. These cycles improved the flow mixing by mobilizing the more stagnant fluid between the plates and in the rectangular cavities. At a Re = 800, the increase in flow rate increased the flow oscillations because the vertical plates directed the main flow toward the rectangular cavities. The flow cycles seen between each plate at a Re = 500 grew even greater at a Re = 800. Smaller velocity vectors leaving the lower part of the main flow were directed to the right and left surfaces of the rectangular cavities, creating flow fluctuations.

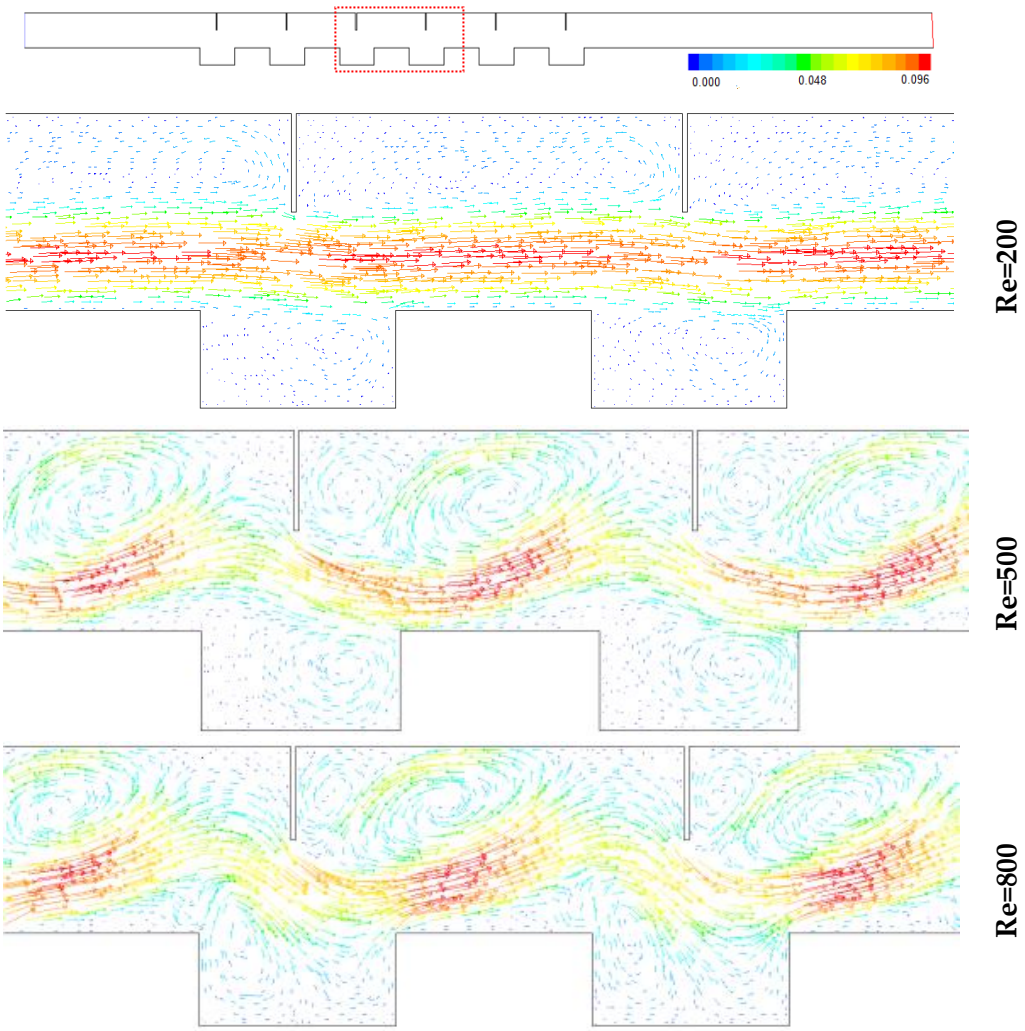

Figure 7. Velocity vectors for varying Re at the steady case of the nanofluid in the channel with plates

Figure 8 displays the velocity fields (a) and temperature contours (b) at varying phase angles in the channel without plates at the Re = 500, A = 1, St = 2, φ = 0.05. It was seen that the velocity and thermal fields changed remarkably by the oscillating parameters and the geometry of the channel. At ωt = 90°, the flow moved downstream and slightly directed into the rectangular cavities due to the oscillating components. At ωt = 180°, the flow began to change direction, and the low velocity fluid particles rotated upstream (in the opposite direction). The flow cycles that occurred in the rectangular cavities became larger. At ωt = 270°, the flow moved completely upstream. Growing flow cycles due to the opposite flow filled the rectangular cavities. At ωt = 360°, the flow began to flow downstream again and the flow cycles in the rectangular cavities got smaller. Thus, one oscillating period was terminated. This case is repeated in each oscillating cycle. The flow cycles that occurred in each periodic cycle carried the hot fluid in the rectangular cavity to the upper sections of the channel. The cold fluid displaced by the hot fluid caused the temperature of the channel walls to diminish. It was observed that the temperature of the channel walls in the oscillating nanofluid flow diminished significantly when compared to the channel wall temperatures in Figure 5b (Fig. 8b).

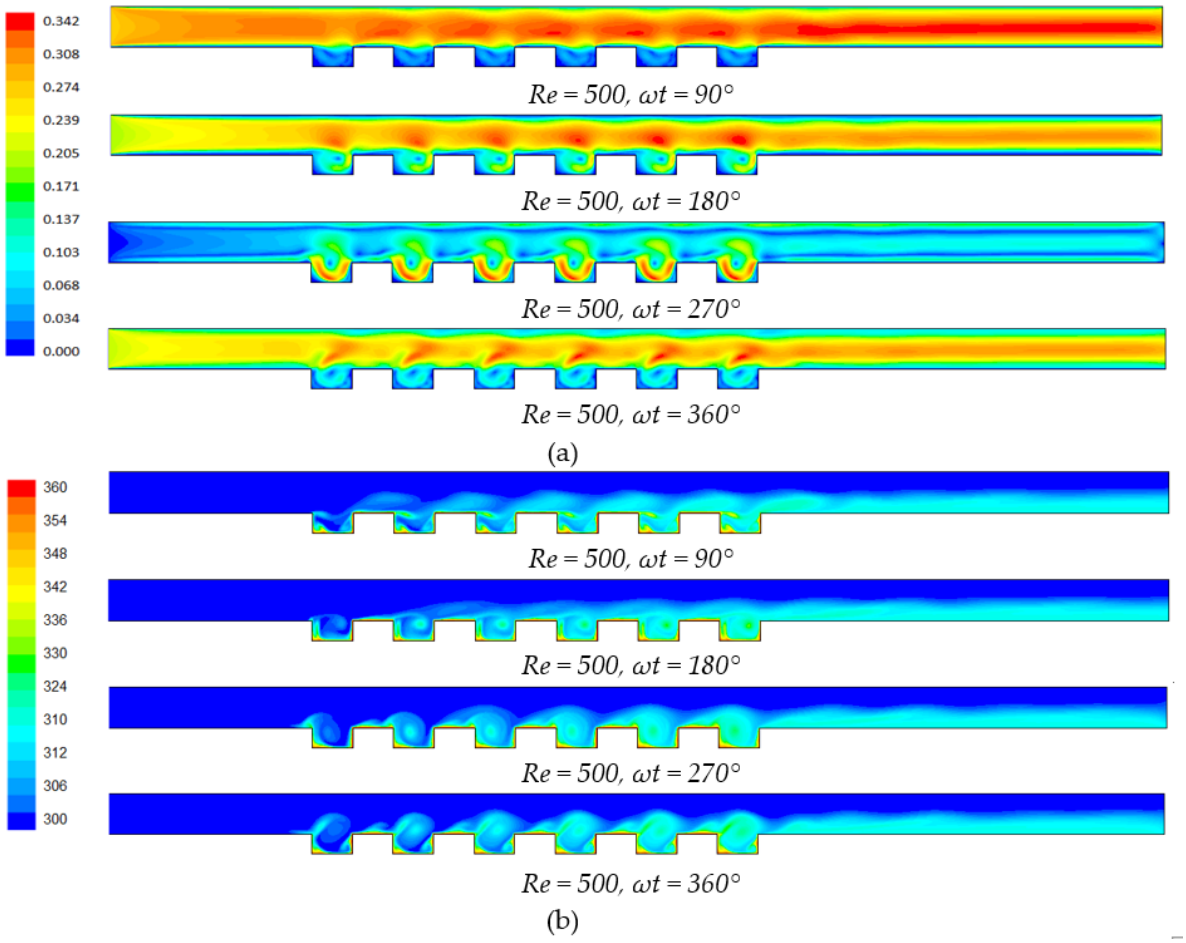

Figure 8. Velocity fields (a) and temperature fields (b) at varying phase angles in the channel without plates (Re = 500, A = 1, St = 2, φ = 0.05)

Figure 9 indicates the velocity fields (a) and temperature structures (b) for an oscillating period in the channel with plates at a Re = 500, A = 1, St = 2, φ = 0.05. The flow and temperature fields varied considerably during one oscillating cycle. The flow flowed downstream at ωt = 90°. The flow was directed into the rectangular cavities due to the vertical plates on the upper wall of the channel. At ωt = 180°, the direction of the flow changed, the fluid particles rotated upstream, and the structure of the flow was completely changed. Wide circulation zones were seen between the plates. Flow cycles also began to form in the rectangular cavities. At ωt = 270°, the flow moved completely upstream. Circular flow cycles were seen all over the channel. The flow began to flow downstream at a phase angle of ωt = 360°. Thus, one oscillating cycle was terminated. The oscillation parameters increased the flow oscillations and flow cycles. This case, which was reiterated in each oscillating cycle, was reflected in the temperature fields and heat transfer enhanced due to the better flow mixture.

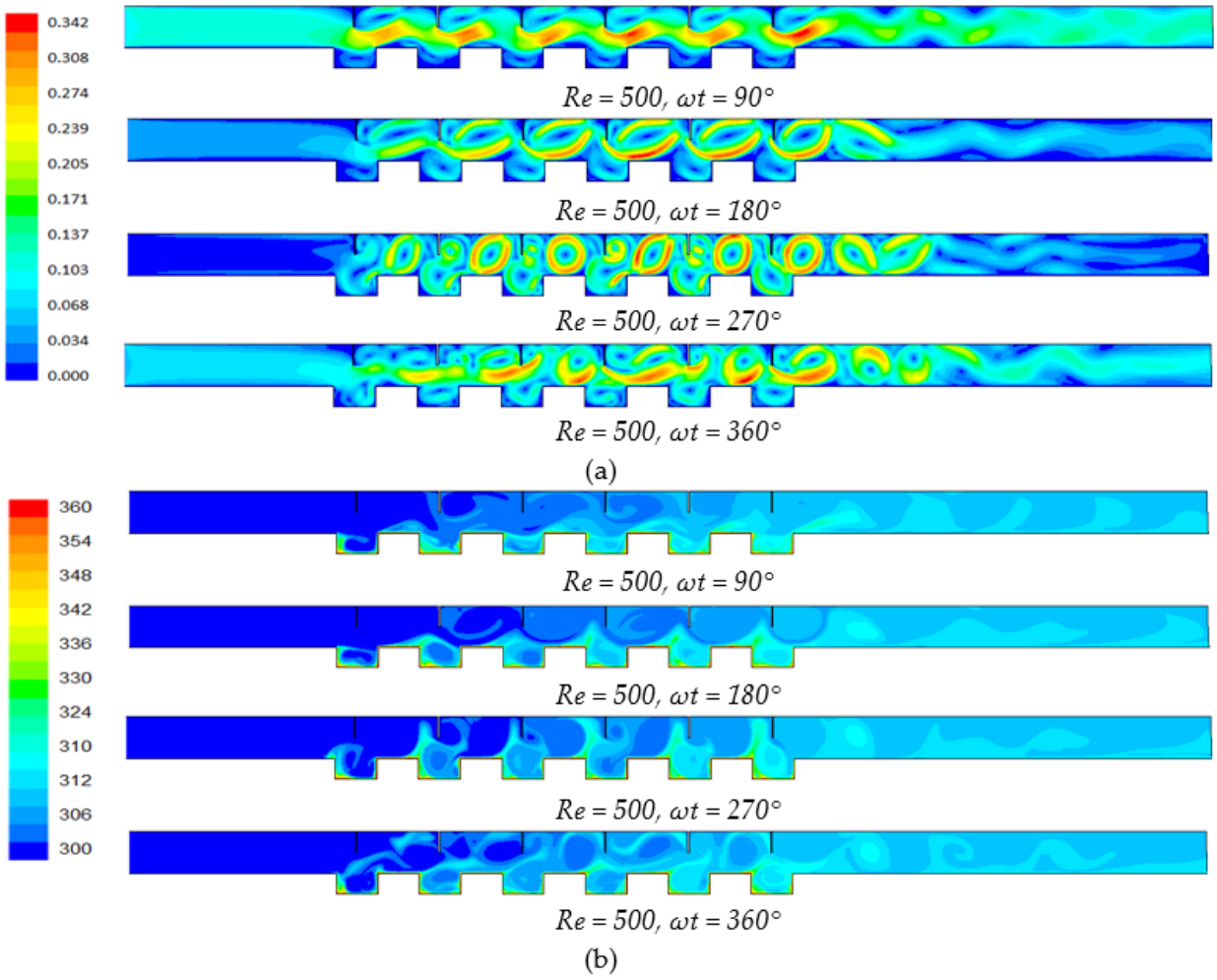

Figure 9. Velocity fields (a) and temperature fields (b) at varying phase angles in the channel with plates (Re = 500, A = 1, St = 2, φ = 0.05)

Figure 10 illustrates the velocity fields (a) and temperature structures (b) of the oscillating nanofluid flow at ωt = 180° for varying Re in the channel without plates. In the upper surfaces of the channel, the flow generally flowed parallel to the surface. Due to the oscillating components, this parallelism was disrupted in the center of the channel and the rectangular cavities on the lower surface, and recirculation zones were formed. With an increasing Re, the recirculation zones enlarged and filled the cavity. These cycles carried the cold fluid from the upper parts of the channel to the hot lower surfaces, thus reducing the temperature of the heated channel surfaces.

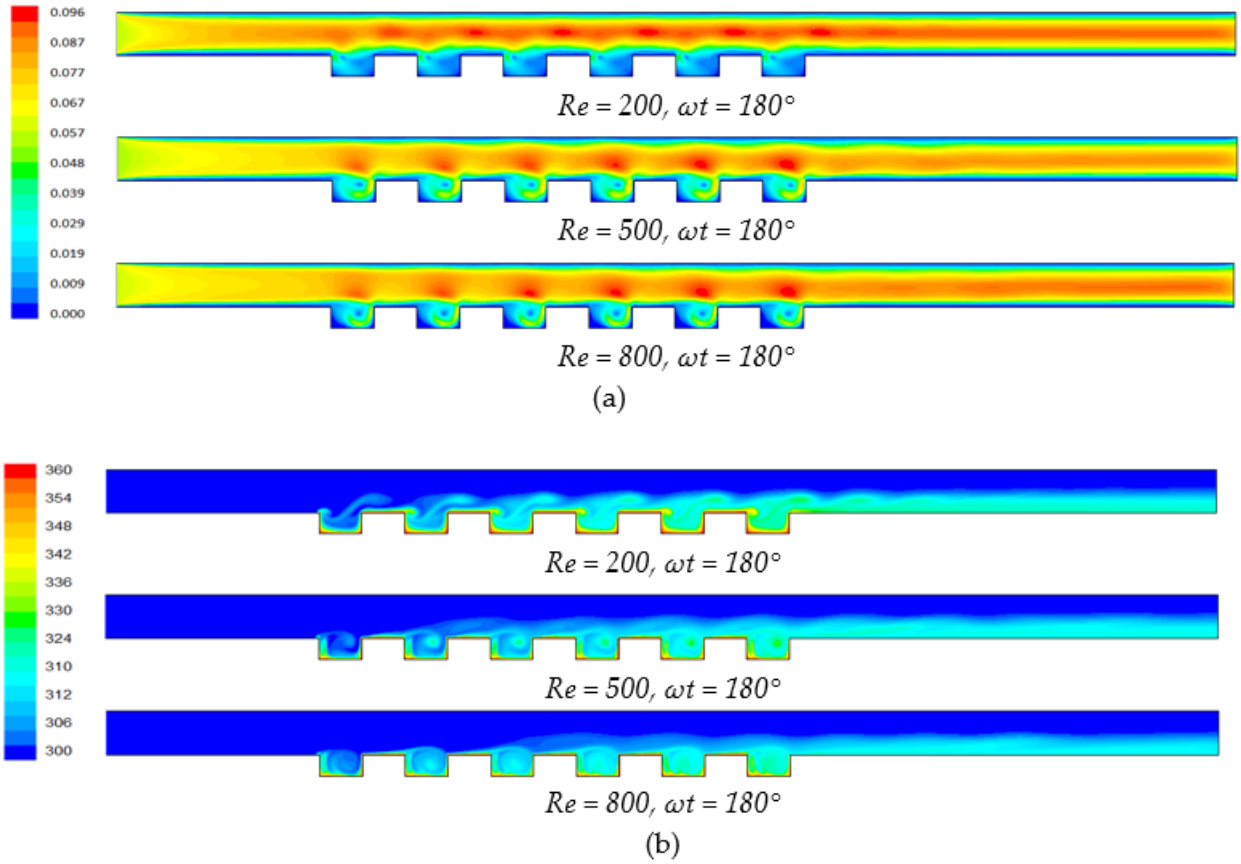

Figure 10. Velocity fields (a), temperature fields (b) at varying Re for oscillating nanofluid flow in the channel without plates (A = 1, St = 2, φ = 0.05, ωt = 180°)

Figure 11 shows the velocity fields (a) and temperature structures (b) of oscillating nanofluid flow at ωt = 180° for different Re in the channel with plates. The vertical plates completely altered the flow fields. The fluid flowed upstream at the ωt = 180° phase angle. Recirculation zones were formed in the channel due to plates and reverse flow. Vortex structures are formed between each plate and in rectangular spaces due to oscillating components. Increasing Re causes an increase in these structures in the channel. The flow cycles that were longitudinal at low Re become circular at high Re. These cycles help move the cold fluid from the top sections of the channel to the heated walls at the lower surface of the channel. Thus, the temperature of the heated walls in contact with the colder fluid diminishes, and heat transfer increases.

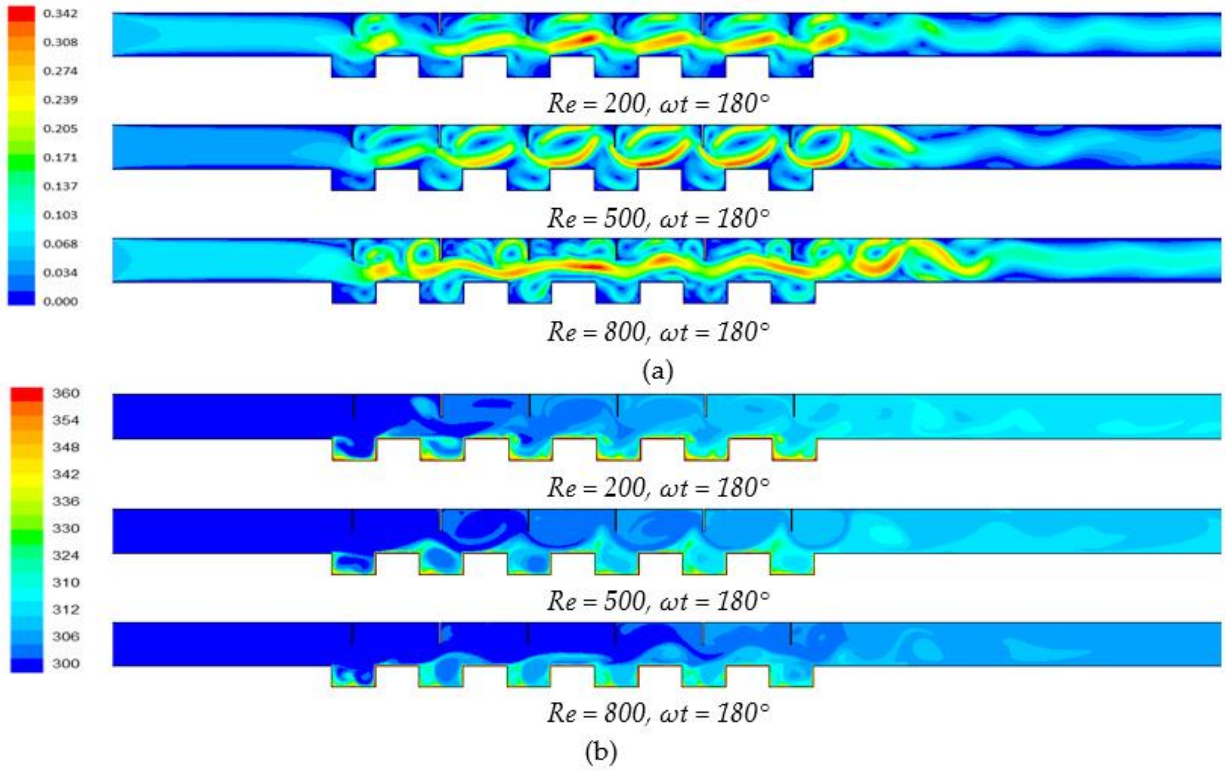

Figure 11. Velocity fields (a) and temperature fields (b) at different Re for the oscillating nanofluid flow in the channel with plates (A = 1, St = 2, φ = 0.05, ωt = 180°)

Figure 12 presents velocity vectors for an oscillating cycle in the channel without plates for Re = 800. At ωt = 90°, the vector directions are downstream. The flow moves parallel to the top surfaces of the channel, and the flow structure is disturbed near the bottom walls. In the corrugated parts of the channel, the vectors are quite small and move freely. At ωt = 180°, the flow starts to reverse direction and only the integrity of the flow is preserved. Flow cycles occurs in rectangular corrugated sections. At ωt = 270°, the direction of the vectors is upstream, and the flow cycles formed in the corrugated sections become larger and wider toward the center of the channel. At ωt = 360°, the vectors begin to flow downstream as a whole, and one cycle is completed.

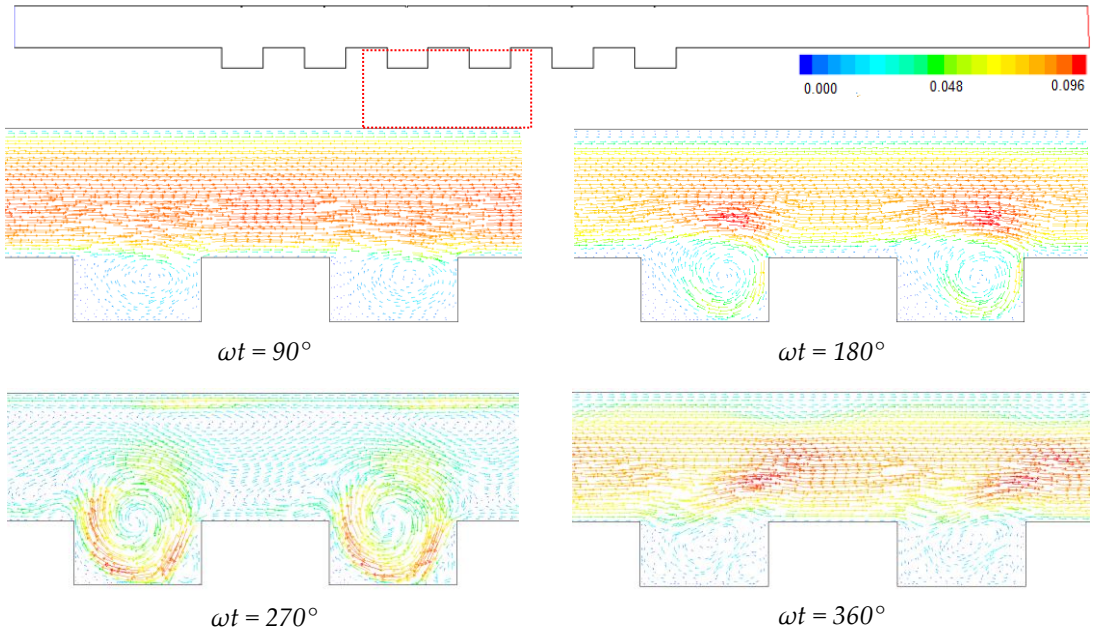

Figure 12. Velocity vectors for one period in the channel without plates at a Re = 800 (A = 1, St = 2, φ = 0.05)

Figure 13 shows the variation of the velocity vectors over one period in the channel with plates. The structure of velocity vectors is quite different from the channel without plates. At ωt = 90°, the main flow is considerably thinner than the channel without plates and flows downstream. The plates and oscillating parameters create flow oscillation. Flow cycles are seen between each plate and in the corrugated parts. At ωt = 180°, the main flow is quite thin, and the velocity vectors rotate upstream. Flow cycles enlarge between the plates and in the corrugated spaces. At ωt = 270°, the direction of the vectors is upstream, and the flow fields are completely disrupted. The recirculation zones grow considerably and spread all over the channel. At ωt = 360°, the flow cycles are lost, and the direction of the vectors is downstream. Thus, one oscillating cycle is completed for the channel with plates.

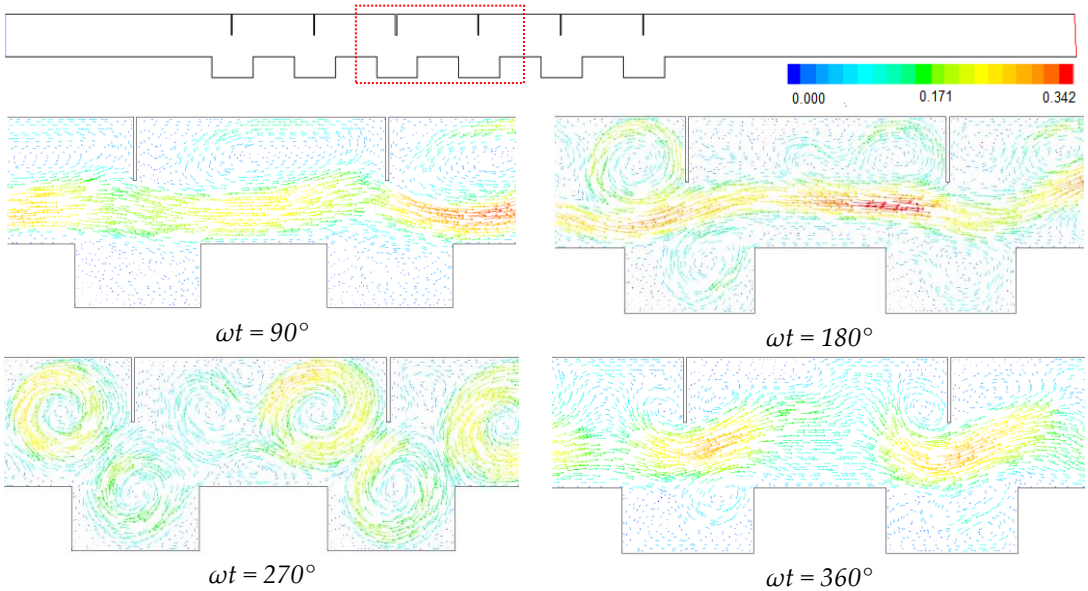

Figure 13. Velocity vectors for one oscillating period in the channel with plates at a Re = 800 (A = 1, St = 2, φ = 0.05)

Figure 14 indicates the variations of the Nu (a), Nu_{rel} (b), f_{rel} (c), and PEC (d) with varying Re for the steady flow. In the Figure, (w), (n), (b, w) and (b, n) subscripts represent the steady flow of the water in the channel without plates, the steady flow of the nanofluid in the channel without plates, the steady flow of water in the channel with plates, and the steady flow of the nanofluid in the channel with plates, respectively. The Nu increased with the rise in the Re for all channel cases. The maximum Nu was obtained as approximately Nu = 39.61 in the steady nanofluid case in the channel with plates at a Re = 800. Nu for the steady case of the nanofluid in the channel with plates increased by about 11% according to the water in the channel without plates.

Figure 14b shows the relative Nusselt number with the Re for oscillating flow of the nanofluid in the channel with/without plates. The Nu_{rel} is compared to the oscillating flow of the nanofluid in the channel with and without plates. (p) and (p, b) subscripts show the oscillating flow of the nanofluid in the channel without plates and with plates, respectively. The Nu_{rel} obtained for the steady state of the water in the channel without plates was considered as a reference. It is seen that the Nu_{rel} increased with the Re. The Nu_{rel} was found to be about 1.39 at the Re = 800 in the channel without plates. The highest Nu_{rel} was acquired at about 1.57 in the channel with plates at the Re = 800.

Figure 14c presents the relative friction factor with the Re for the oscillating flow of the nanofluid in the channel with and without plates. Since the plates added into the channel prevent the flow, the pressure loss in the channel increases. In addition, since the viscosity values of nanofluids is high than the basic fluid, it causes an increase in the pressure drop. Therefore, an important pressure loss occurred in the channel due to the plates, nanoparticles, and oscillating parameters. In Figure 14c, (p, b), (p) and (w) subscripts indicate the oscillating flow of the nanofluid in the channel with plates, the oscillating flow of the nanofluid in the channel without plates, and the steady flow of water in the channel without plates, respectively. The relative friction factor obtained in the steady flow of the water in the channel without plates was considered as a reference. It is seen that the f_{rel} increased with the Re. The relative friction factor was achieved at about 2.53 in the channel without plates at a Re = 800. The highest f_{rel} was acquired at nearly 3.82 in the channel with plates at a Re = 800.

Figure 14d indicates the variation of the PEC with the Re for the oscillating flow of the nanofluid in the channel with and without plates. In Figure 14d, PEC (p, b), PEC (p) and PEC (w) indicate performance evaluation criteria for the oscillating flow of the nanofluid in the channel with plates, for the oscillating flow of the nanofluid in the channel without plates, and for the steady flow of water in the channel without plates, respectively. The PEC obtained in the steady case of the water in the channel without plates was considered as a reference. Depending on the Nu_{rel} and f_{rel}, PEC was calculated in Eq. (16). PEC value higher than 1 show that the heat transfer in the channel is higher than the pressure drop. The PEC values were found very close to each other in all the tested Re. Although the Nu_{rel} was high in the channel with plates, the PEC values were almost the same for all the Re due to the increased the f_{rel}. The best PEC was achieved as 1.046 at a Re = 200 in the channel without plates. At the Re =200, the f_{rel} was very low in the channel without plates.

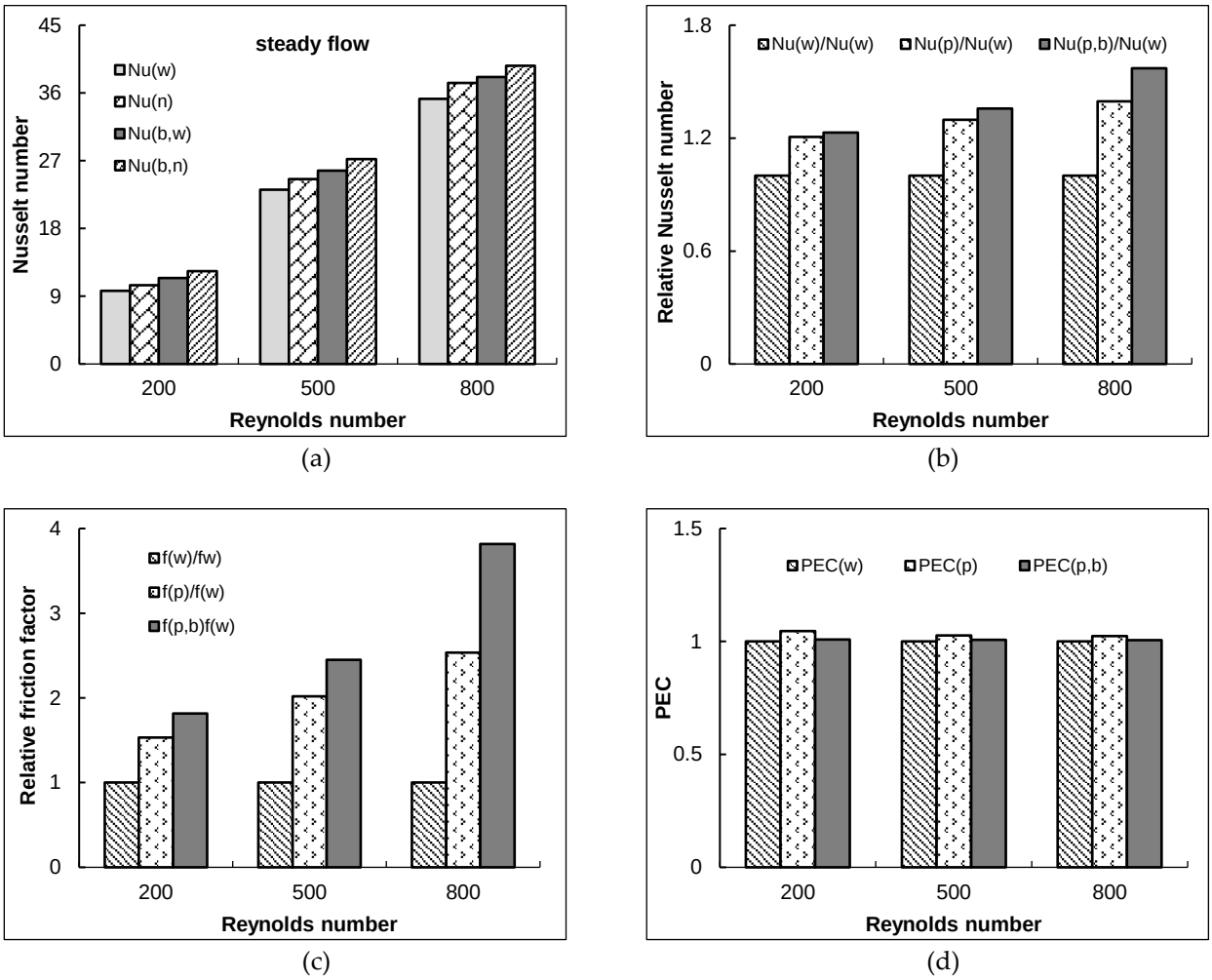

Figure 14. Nu for the steady flow (a), Nu_{rel} (b), f_{rel} (c), and PEC (d) with the Re

Figure 15 indicates the variation of the Nu with one oscillating cycle for the nanofluid flow at varying Re, in the channel without plates (a) and in the channel with plates (b). As can be seen from both figures, the Nu changed into sinusoidal form for one oscillating cycle in all the studied Re. As the Re increased, the Nu also increased. Moreover, the range of variation of the Nu was small at a low Re and larger at a high Re. It was seen that the Nu achieved in the channel with plates was higher than without plates. One pulsating cycle is completed at $\omega t=2\pi=360°$. The curve of the Nusselt number changes sinusoidally over the course of one cycle due to the pulsating velocity input. The pulsating flow mechanism throughout one cycle is explained in detail in the Figures 8 and 9. While the flow moves in the downstream direction until the phase angle $\omega t = 180°$, after $\omega t = 180°$ the direction of the flow changes and it starts to flow in the upward direction. At $\omega t =270°$, the flow direction is towards the channel entrance. A decrease in the Nusselt number is observed at this phase angle due to the movement of the hotter fluid at the channel exit towards the channel entrance. After the phase angle $\omega t =270°$, the flow changes direction again and starts to flow towards the channel exit. As the colder fluid at the channel entrance joins the pulsating cycle, the Nusselt number begins to increase.

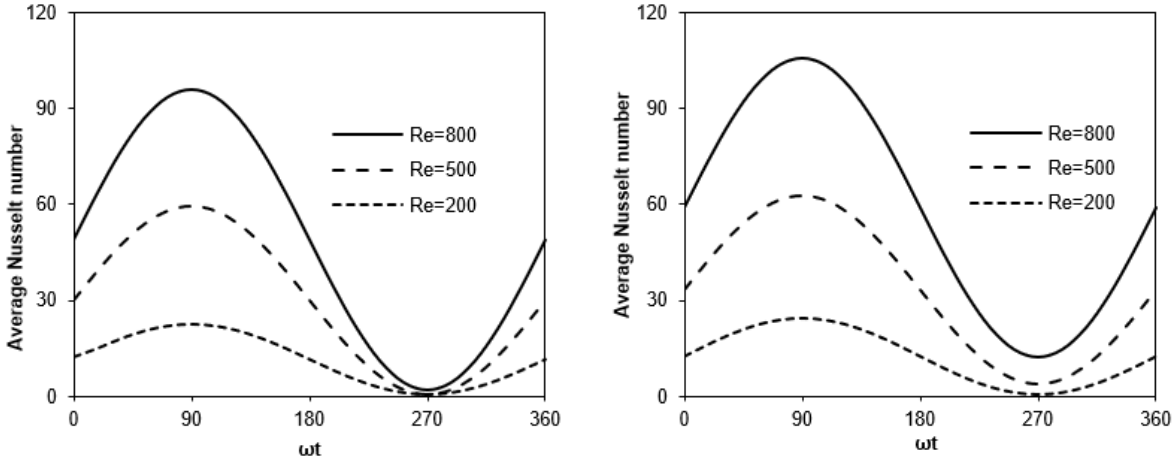

Figure 15. Nu with phase angles for the oscillating nanofluid flow at varying Re

The findings obtained from this study were compared with previous studies [44] to support them with literature studies. The parameters used in both studies are given in Table 2. In both studies, Nu_{rel}, f_{rel} and PEC values obtained under pulsating nanofluid flow conditions in the channel with vertical plates were presented in Table 3. f_{rel} values obtained in this study were found to be lower than [44]. It is seen that Nu_{rel} and PEC values were obtained higher in [44] than in this study. The reason for this may be due to differences between the parameters used in both studies.

Table 2 . Comparison of the parameters used in this study and [44]

Reference	Wave type	D_h	Re	A	St	T_i	T_w	Fluid	φ
Ref. [44]	Circular	12mm	200, 500, 800	1	2	293K	350K	CuO-water	3%
Present study	Rectangular	12mm	200, 500, 800	1	2	300K	360K	Al_2O_3-water	5%

Table 3 . Comparison of the results obtained from this study and [44]

Reference	Re	Nu_{rel}	f_{rel}	PEC
Ref. [44]	200	2.624	3.014	1.817
	500	2.581	3.185	1.752
	800	2.640	3.467	1.744
Present study	200	1.230	1.816	1.008
	500	1.358	2.451	1.007
	800	1.572	3.818	1.006

Present study indicates that the use of plates in the grooved channels significantly influences the flow behavior and heat transfer. Furthermore, preferring nanofluids as the working fluid increases the thermal enhancement relative to the base fluid. Additionally, the oscillating flow, when compared to the steady flow, considerably raises the heat transfer as it creates better flow mixing. Flow oscillations keep the nanoparticles in continuous motion in the channel and prevent the particles from collapsing. Therefore, it is very advantageous to use oscillating flow in nanofluid flows. However, the pump power in the channel slightly increases due to the plates, nanoparticles, and oscillating flow.

4. CONCLUSIONS

This numerical work examined the effects of the oscillating flow of the Al_2O_3-water nanofluid on the thermohydraulic performance in a rectangular corrugated channel with/without plate. The results

compared to steady case of the water in the channel with/without plates. The thermal performance and hydraulic behaviors of the vertical plates, Al_2O_3-water nanofluid, oscillating components, and Re were investigated. The temperature and flow fields in the channel were obtained for varying parameters. The pronounced consequences of the present work were presented by:

- The temperature and flow fields were significantly changed by the channel geometry, vertical plates, and oscillating components. The oscillating flow occurred due to the vertical plates and oscillating parameters, creating circulation zones between the plates and in the rectangular corrugated parts.
- Al_2O_3-water nanofluid increased Nusselt number compared to base fluid (water).
- The oscillating parameters provided important thermal enhancement in comparison with steady cases. The highest thermal enhancement was about 1.57 for the oscillating nanofluid flow at a Re = 800 in the channel with plates.
- The heat transfer increased with Re for all the cases. The Nu varied sinusoidally during one oscillating cycle, and the changing range of Nu increased with an increasing Re.
- The PEC values were obtained close to each other for all the tested Re.
- The pressure loss increased in the channel due to the plates, nanoparticles, oscillating amplitude, and oscillating frequency. The highest f_{rel} was found as about 3.82 in the channel with plates for the oscillating nanofluid flow at the Re = 800.
- Present study proved that the combinations of plates, nanofluids, and oscillating flow in the corrugated channels have important potential for thermal improvement.
- In future studies, the effects of different nanoparticle types and different nanoparticle volume ratios on flow and heat transfer can be investigated by changing the lengths and angles of the plates.

Declaration of Ethical Standards

The author declares that all ethical guidelines including authorship, citation, data reporting, and publishing original research are followed.

Declaration of Competing Interest

The author declares that there is no conflict of interest.

Funding / Acknowledgements

This study did not receive funding from any provider.

REFERENCES

[1] T. Alam, R. P. Saini, and J. S. Saini, "Use of turbulators for heat transfer augmentation in an air duct–A Review," *Renew. Energy*, vol. 62, pp. 689-715, 2014. https://doi.org/10.1016/j.renene.2013.08.024

[2] F. Menasria, M. Zedairia, and A. Moummi, "Numerical study of thermohydraulic performance of solar air heater duct equipped with novel continuous rectangular plates with high aspect ratio," *Energy*, vol. 133, pp. 593-608, 2017. https://doi.org/10.1016/j.energy.2017.05.002

[3] X. Gu, Z. Zheng, X. Xiong, E Jiang, T. Wang, D. Zhang, "Heat transfer and flow resistance characteristics of helical baffle heat exchangers with twisted oval tube," *Journal of Thermal Science*, vol. 31, no. 2, pp. 370–378, 2022. https://doi.org/10.1007/s11630-022-1581-1

[4] P. Naphon, and K. Kornkumjayrit, "Numerical analysis on the fluid flow and heat transfer in the channel with V-shaped wavy lower plate," *Int. Commun. Heat Mass Transfer*, vol. 35, pp. 839-843, 2008. https://doi.org/10.1016/j.icheatmasstransfer.2008.03.010

[5] N. E. Davkhar, and N. K. Deshmukh, "Review on analysis of heat transfer and fluid flow characteristics in corrugated duct," *International Journal of Research Publication and Reviews*, vol. 2, no. 1, pp. 262-268, 2021.

[6] H. Zontul, H. Hamzah, N. Kurtulmus, B. Sahin, "Investigation of convective heat transfer and flow hydrodynamics in rectangular grooved channels, *Int. Commun. Heat Mass Transfer*, vol. 126, no. 105366, 2021. https://doi.org/10.1016/j.icheatmasstransfer.2021.105366

[7] N. Kurtulmus, and B. Sahin, "A Review of hydrodynamics and heat transfer through corrugated channels," *Int. Commun. Heat Mass Transfer*, vol. 108, p. 104307, 2019. https://doi.org/10.1016/j.icheatmasstransfer.2019.104307

[8] Z. Brodnianská, and S. Kotśmíd, "Intensification of convective heat transfer in new shaped wavy channel configurations," *Int. J. Therm. Sci.,* vol. 162, p. 106794, 2021. https://doi.org/10.1016/j.ijthermalsci.2020.106794

[9] S. K. Mehta, S. Pati, and L. Baranyi, "Effect of amplitude of walls on thermal and hydrodynamic characteristics of laminar flow through an asymmetric wavy channel," *Case Stud. Therm. Eng.,* vol. 31, p. 101796, 2022. https://doi.org/10.1016/j.csite.2022.101796

[10] S. Skullong, P. Promvonge, C. Thianpong, M. Pimsarn, "Thermal performance in solar air heater channel with combined wavy-groove and perforated-delta wing vortex generators," *Appl. Therm. Eng.,* vol. 100, pp. 611–620, 2016. https://doi.org/10.1016/j.applthermaleng.2016.01.107

[11] M. A. El-Habet, S. A. Ahmed, and M. A. Saleh, "The effect of using staggered and partially tilted perforated baffles on heat transfer and flow characteristics in a rectangular channel," *Int. J. Therm. Sci.,* vol. 174, p. 107422, 2022. https://doi.org/10.1016/j.ijthermalsci.2021.107422

[12] Y. G. Lei, Y. L. He, and R. Li, "Effects of baffle inclination angle on flow and heat transfer of a heat exchanger with helical baffles," *Chem. Eng. Process. Process. Intensif.,* vol. 47, no. 12, pp. 2336–2345, 2008. https://doi.org/10.1016/j.cep.2008.01.012

[13] S. Sripattanapipat, and P. Promvonge, "Numerical analysis of laminar heat transfer in a channel with diamond-shaped baffles," *Int. Commun. Heat Mass Transfer*., vol. 36, no. 1, pp. 32-38, 2009. https://doi.org/10.1016/j.icheatmasstransfer.2008.09.008

[14] S. Kwankaomeng, and P. Promvonge, "Numerical prediction on laminar heat transfer in square duct with 30° angled baffle on one wall," *Int. Commun. Heat Mass Transfer*, vol. 37, pp. 857-866, 2010. https://doi.org/10.1016/j.icheatmasstransfer.2010.05.005

[15] P. Sriromreun, "Numerical study on heat transfer enhancement in a rectangular duct with incline shaped baffles," *Chem. Eng. Transfer*, vol. 57, pp. 1243–1248, 2017. https://doi.org/10.3303/CET1757208

[16] Z. Li, and Y. Gao, "Numerical study of turbulent flow and heat transfer in cross corrugated triangular ducts with delta-shaped baffles," *Int. J. Heat Mass Transfer*, vol. 108, pp. 658–670, 2017. https://doi.org/10.1016/j.ijheatmasstransfer.2016.12.054

[17] K. Karabulut, "Heat transfer and pressure drop evaluation of different triangular baffle placement angles in cross-corrugated triangular channels," *Therm. Sci*., 2020, vol. 24, pp. 355-365. https://doi.org/10.2298/TSCI190813466K

[18] C. E. Bensaci, A. Moummi, F.J. Sanchez de la Flor, E.A. Rodriguez Jara, A. Rincon-Casado, A. Ruiz-Pardo, "Numerical and experimental study of the heat transfer and hydraulic performance of solar air heaters with different baffle positions," *Renew. Energy*, vol. 155, pp. 1231–1244, 2020. https://doi.org/10.1016/j.renene.2020.04.017

[19] P. Promvonge, S. Tamna, M. Pimsarn, C. Thianpong, "Thermal characterization in a circular tube fitted with inclined horseshoe baffles," *Appl. Therm. Eng.,* vol. 75, pp. 1147–1155, 2015. https://doi.org/10.1016/j.applthermaleng.2014.10.045

[20] R. Kumar, A. Kumar, R. Chauhan, M. Sethi, "Heat transfer enhancement in solar air channel with broken multiple V-type baffle," *Case Stud. Therm. Eng*. vol. 8, pp. 187–197, 2016. https://doi.org/10.1016/j.csite.2016.07.001

[21] D. Sahel, H. Ameur, R. Benzeguir, Y. Kamla, "Enhancement of heat transfer in a rectangular

channel with perforated baffles," *Appl. Therm. Eng.*, vol. 101, pp. 156–164, 2016. https://doi.org/10.1016/j.applthermaleng.2016.02.136

[22] A. M. Abed, M. A. Alghoul, K. Sopian, H.A. Mohammed, H. Majdi, A.N. Alshamani, "Design characteristics of corrugated trapezoidal plate heat exchangers using nanofluids," *Chem. Eng. Process. Process. Intensif.*, vol. 87, pp. 88–103. 2015. https://doi.org/10.1016/j.cep.2014.11.005

[23] H. Fazeli, S. Madani, and P. R. Mashaei, "Nanofluid forced convection in entrance region of a baffled channel considering nanoparticle migration," *Appl. Therm. Eng*., vol. 106, pp. 293–306, 2016. https://doi.org/10.1016/j.applthermaleng.2016.06.010

[24] O. A. Alawi , H. M. Kamar , O. A. Hussein, A. R. Mallah, H. A. Mohammed, M. Khiadani, A. B. Roomi, S. N. Kazi , Z. M. Yaseen, "Effects of binary hybrid nanofluid on heat transfer and fluid flow in a triangular-corrugated channel: An experimental and numerical study," *Powder Technology*, vol. 395, pp. 267-279, 2022. https://doi.org/10.1016/j.powtec.2021.09.046

[25] O. Manca, S. Nardini, and D. Ricci, "A Numerical study of nanofluid forced convection in ribbed channels," *Appl. Therm. Eng.*, vol. 37, pp. 280-297, 2012. https://doi.org/10.1016/j.applthermaleng.2011.11.030

[26] A. Heshmati, H. A. Mohammed, and A. N. Darus, "Mixed convection heat transfer of nanofluids over backward facing step with a slotted baffle," *Applied Mathematics and Computation*, vol. 240, pp. 368–386, 2014. https://doi.org/10.1016/j.amc.2014.04.058

[27] G. Huminic, and A. Huminic. "Heat transfer and flow characteristics of conventional fluids and nanofluids in curved tubes: A review," *Renewable and Sustainable Energy Reviews*. vol. 58, pp. 1327–1347, 2016. https://doi.org/10.1016/j.rser.2015.12.230

[28] C. Qi, Y. L. Wan, C. Y. Li, D.T. Han, Z.H. Rao, "Experimental and numerical research on the flow and heat transfer characteristics of TiO_2-water nanofluids in a corrugated tube," *Int. J. Heat Mass Transfer*, vol. 115, pp. 1072–1084, 2017. https://doi.org/10.1016/j.ijheatmasstransfer.2017.08.098

[29] A. H. Pordanjani, S. Aghakhani, M. Afrand, B. Mahmoudi, O. Mahian, S. Wongwises, "An updated review on application of nanofluids in heat exchangers for saving energy," *Energy Conversion Management*, vol. 198, p. 111886, 2019. https://doi.org/10.1016/j.enconman.2019.111886

[30] S. Mei, C. Qi, T. Luo, X. Zhai, Y. Yan, "Effects of magnetic field on thermo-hydraulic performance of Fe_3O_4-water nanofluids in a corrugated tube," *Int. J. Heat Mass Transfer*, vol. 128, pp. 24–45, 2019. https://doi.org/10.1016/j.ijheatmasstransfer.2018.08.071

[31] A. Kaood, and M. A. Hassan, "Thermo-hydraulic performance of nanofluids flow in various internally corrugated tubes," *Chem. Eng. Process. Process. Intensif.*, vol. 154, p. 08043, 2020. https://doi.org/10.1016/j.cep.2020.108043

[32] M-W. Tian, S. Khorasani, H. Moria, S, Pourhedayat, H.S. Dizaji, "Profit and efficiency boost of triangular vortex-generators by novel techniques," *Int. J. Heat Mass Transfer*, vol. 156, p. 19842, 2020. https://doi.org/10.1016/j.ijheatmasstransfer.2020.119842

[33] R. K. Ajeel, K. Sopian, and R. Zulkifli, "Thermal-hydraulic performance and design parameters in a curved-corrugated channel with L-shaped baffles and nanofluid," *Journal of Energy Storage*, vol. 34, p. 101996, 2021. https://doi.org/10.1016/j.est.2020.101996

[34] S. Akcay, and U. Akdag, "Heat transfer enhancement in a channel with inclined baffles under pulsating flow: A CFD study," *Journal of Enhanced Heat Transfer*, vol. 30, no. 5, pp. 61-79, 2023. https://doi.org/10.1615/JEnhHeatTransf.2023047227

[35] Y. Menni, A. J. Chamkha, M. Ghazvini, M.H. Ahmadi, H. Ameur, A. Issakhov, M. Inc, "Enhancement of the turbulent convective heat transfer in channels through the baffling technique and oil/multiwalled carbon nanotube nanofluids," *Numerical Heat Transfer, Part A: Applications*, vol. 79, no. 4, pp. 311-351, 2021. https://doi.org/10.1080/10407782.2020.1842846

[36] U. Akdag, S. Akcay, and D. Demiral, "Heat transfer enhancement with laminar pulsating nanofluid flow in a wavy channel," *Int. Commun. Heat Mass Transfer*, vol. 59, pp. 17–23, 2014. https://doi.org/10.1016/j.icheatmasstransfer.2014.10.008

[37] S. W. Chang, and T. H. Cheng, "Thermal performance of channel flow with detached and attached pin-fins of hybrid shapes under inlet flow pulsation," *Int. J. Heat Mass Transfer*, vol. 164, p. 20554, 2021. https://doi.org/10.1016/j.ijheatmasstransfer.2020.120554

[38] Akcay, S. "Numerical analysis of hydraulic and thermal performance of Al_2O_3-water nanofluid in a zigzag channel with central winglets," *Gazi University Journal of Science*, vol. 36, pp. 383-397, 2023. https://doi.org/10.35378/gujs.1012201

[39] U. Akdag, S. Akcay, and D. Demiral, "Heat transfer in a triangular wavy channel with CuO-water nanofluids under pulsating flow," *Therm. Sci.,* vol. 23, no. 1, pp. 191-205, 2019. https://doi.org/10.2298/TSCI161018015A

[40] U. Akdag, S. Akcay, and D. Demiral, "Heat transfer enhancement with nanofluids under laminar pulsating flow in a trapezoidal-corrugated channel," *Progress in Computational Fluid Dynamics,* vol. 17, no. 5, pp. 302-312, 2017. https://doi.org/10.1504/PCFD.2017.086322

[41] M.H. Esfe, M. Bahiraei, A. Torabi, M. Valadkhani, "A critical review on pulsating flow in conventional fluids and nanofluids: thermo-hydraulic characteristics," *Int. Commun. Heat Mass Transfer*., vol. 120, p. 104859, 2021. https://doi.org/10.1016/j.icheatmasstransfer.2020.104859

[42] J. Munoz-Camara, D. Crespí-Llorens, J.P. Solano, P. Vicente, "Baffled tubes with superimposed oscillatory flow: Experimental study of the fluid mixing and heat transfer at low net Reynolds numbers," *Experimental Thermal and Fluid Science*, vol. 123, p. 110324, 2021. https://doi.org/10.1016/j.expthermflusci.2020.110324

[43] S. Akcay, "Numerical analysis of heat transfer ımprovement for pulsating flow in a periodic corrugated channel with discrete V-type winglets," *Int. Commun. Heat Mass Transfer*, vol. 134, p. 105991, 2022. https://doi.org/10.1016/j.icheatmasstransfer.2022.105991

[44] S. Akcay, "Heat transfer analysis of pulsating nanofluid flow in a semicircular wavy channel with baffles," *Sādhanā*, vol. 48, no. 2, pp. 57, 2023. https://doi.org/10.1007/s12046-023-02119-x

[45] S. Kakac, and A. Pramuanjaroenkij, "Review of convective heat transfer enhancement with nanofluids," *Int. J. Heat Mass Transfer,* vol. 52, pp. 3187–3196, 2009. https://doi.org/10.1016/j.ijheatmasstransfer.2009.02.006

[46] ANSYS Inc. ANSYS Fluent User Guide & Theory Guide-Release 15.0 USA, 2015.

[47] K. Boukhadia, H. Ameur, D. Sahel, M. Bozit, "Effect of the perforation design on the fluid flow and heat transfer characteristics of a plate fin heat exchanger," *Int. J. Therm. Sci*., vol. 126, pp. 172-180, 2018. https://doi.org/10.1016/j.ijthermalsci.2017.12.025

[48] H. Ameur, D. Sahel, and Y. Menni, "Numerical investigation of the performance of perforated baffles in a plate-fin heat exchanger," *Therm. Sci*., vol. 25, no. 5B, pp. 3629-3641, 2021. https://doi.org/10.2298/TSCI190316090A